Physicochem. Probl. Miner. Process., 62(5), 2026, 235920 | Physicochemical Problems of Mineral Processing

http://www.journalssystem.com/ppmp

ISSN 1643-1049

Upgrading of low-grade titanium ores by high-intensity magnetic separation: A case study from Eskişehir, Türkiye

Ulas Uslu, Yusuf Enes Pural, Mustafa Özer

Istanbul Technical University, Faculty of Mines, Mineral Processing Engineering Department, 34469, Maslak, Istanbul, TÜRKİYE

Corresponding authors: usluu19@itu.edu.tr (Ulas Uslu), ozermust@itu.edu.tr (Mustafa Özer)

Abstract: Titanium is a strategic critical raw material whose supply is dominated by ilmenite and rutile-rich heavy mineral sands and leaving fine-grained, hard rock occurrences largely unexploited. This study presents the first systematic physical beneficiation investigation of a representative primary titanium ore from the Eskişehir region (northwestern Türkiye), in which titanium is hosted predominantly by non-magnetic titanite (sphene) and rutile intimately intergrown with an iron rich silicate–oxide gangue. The run-of-mine ore, grading 4.07% TiO_2 in a matrix dominated by SiO_2 (36.09%) and Fe_2O_3 (24.11%), was characterized by XRF, polarized light microscopy, and XRD, and upgraded through a reverse magnetic separation approach in which the iron-bearing gangue is rejected into the magnetic fraction. Magnetic separation tests across a range of particle sizes revealed a strongly liberation-controlled response, with effective separation achieved only below 0.106 mm. Under optimum conditions—ore ground to 100% passing 0.106 mm and processed in a two-stage Carpco wet high-intensity magnetic separator (WHIMS) at 7,000 and 11,000 Gauss—a non-magnetic concentrate grading 12.78% TiO_2 was obtained at a recovery of 53.7%, representing an approximately threefold upgrade while rejecting 95.4% of the total iron into the tailings. Semi-quantitative XRD confirmed titanite (23.9 wt%) as the dominant titanium-bearing phase, with ilmenite limited to only 3.1%, demonstrating the high selectivity of the reverse separation strategy. The results establish an effective, reagent-free pre-concentration route for Eskişehir primary titanium ores and provide a mineralogically grounded basis for the further metallurgical development of Türkiye's domestic hard-rock titanium resources.

Keywords: titanium, titanite (sphene), reverse magnetic separation, physical beneficiation

1. Introduction

Titanium is a strategic transition metal valued across the aerospace, defence, marine, chemical and biomedical industries for its high specific strength, corrosion resistance, biocompatibility and high-temperature stability. The greater part of mined titanium, however, is consumed not as metal but as titanium dioxide (TiO_2) pigment, which underpins the paint, coating, plastic and paper industries (Gázquez et al., 2014). The combination of high economic importance, a geographically concentrated supply base and persistent supply-chain vulnerability has placed titanium firmly on the principal raw-material criticality lists: it is designated both a critical and a strategic raw material under the European Critical Raw Materials Act, which entered into force on 23 May 2024 and identifies 34 critical and 17 strategic raw materials (European Commission, 2024), and it is one of the twelve defence-critical raw materials listed by NATO in December 2024 (NATO, 2024). These designations, together with the limited domestic primary capacity of most consuming regions, have intensified interest in recovering titanium from unconventional and low-grade resources and in improving circularity along the value chain (European Commission Joint Research Centre, 2025).

Among the primary titanium minerals, rutile (TiO_2), ilmenite ($FeTiO_3$) and titanite, or sphene ($CaTiSiO_5$), are the most important, with rutile commanding the highest value: the mineral is stoichiometrically pure TiO_2, and natural rutile typically grades 93–96% TiO_2. Ilmenite, which carries the bulk of world titanium production, contains 52.6% TiO_2 and exhibits moderate paramagnetism as a result of its structural iron, whereas titanite

DOI: 10.37190/ppmp/235920

contains up to about 40% TiO_2 but hosts essentially no structural iron and is therefore diamagnetic (Gázquez et al., 2014). Despite its wide distribution in alkaline and metasomatic igneous environments, titanite has historically been under-exploited, both because of its comparatively low titanium content and because of the difficulty of separating it from chemically and physically similar calc-silicate gangue.

Conventional titanium production is dominated by ilmenite and rutile-rich heavy-mineral sands, in which the titanium-bearing grains are coarse, well liberated and concentrated through a well-established physical flowsheet. Gravity pre-concentration on spirals, shaking tables and Reichert cones first exploits the density contrast between the heavy minerals and the quartz-dominated gangue (Nzeh et al., 2023); low- and high-intensity magnetic separation then fractionates paramagnetic ilmenite from non-magnetic rutile and zircon, and electrostatic (high-tension) separation completes the split on the basis of surface conductivity (Nzeh and Popoola, 2024). For finer or more complex feeds, froth flotation with fatty-acid or amine collectors is applied as a complementary route (Chen et al., 2021). These flowsheets were nevertheless developed for unconsolidated sands in which titanium reports to coarse, liberated grains that are either strongly paramagnetic (ilmenite) or highly conductive (rutile, zircon). Hard-rock, alkaline-related deposits present a fundamentally different problem: titanium is hosted in fine-grained, diamagnetic to weakly magnetic rutile and titanite that are intimately intergrown with iron-bearing silicates and oxides, which renders both density and conductivity based routes largely ineffective.

Magnetic separation is therefore the cornerstone technique for such ores, discriminating minerals according to their differing magnetic susceptibilities. Strongly magnetic phases such as magnetite and titanomagnetite are readily rejected by low-intensity magnetic separation (LIMS), whereas the recovery of paramagnetic ilmenite from weakly magnetic or diamagnetic gangue requires high-intensity (HIMS) or high-gradient magnetic separation (HGMS); modern wet high-gradient and magnetic–gravity systems have substantially improved the treatment of fine, iron-bearing titanium minerals in complex silicate matrices (Opalev et al., 2026). The grade and recovery attainable from such fine-grained ores are, however, governed primarily by liberation: unless the titanium-bearing phases are physically detached from the gangue, no magnetic circuit can separate them effectively, and the achievable enrichment ratio is set by the degree of liberation reached during comminution (Liu et al., 2025).

When the target titanium minerals are rutile and titanite—both of which lack the structural iron required to generate a strong paramagnetic response—the separation logic must be inverted. In this reverse magnetic separation configuration, high-intensity magnetic separation is used not to recover the valuable phase but to draw the dense, iron-bearing gangue (hematite, magnetite and iron-rich silicates) into the magnetic fraction, so that the diamagnetic to weakly magnetic TiO_2 minerals are upgraded in the non-magnetic product. This reagent-free, physical pre-concentration route is increasingly favoured for weakly magnetic and diamagnetic titanium minerals in low-grade deposits, where it avoids the high reagent consumption of chemical upgrading (Fawzy et al., 2025).

The Eskişehir region of north-western Türkiye offers a geologically favourable setting for such unconventional titanium resources. The region is characterised by widespread Cenozoic alkaline magmatism and hosts complex alkaline silicate–carbonatite diatremes, where intense hydrothermal alteration and metasomatism have produced mineral assemblages enriched in plagioclase, orthoclase, bastnäsite, fluorite and barite (Ersoy et al., 2025). Reconnaissance sampling of these primary deposits has indicated titanium mineralisation hosted chiefly by rutile and titanite, with average TiO_2 grades of 4–6%.

The present study reports, to the best of the authors' knowledge, the first systematic physical-beneficiation investigation of a representative hard-rock titanium ore from the Eskişehir primary deposit. The specific objectives are: (i) to characterise the ore mineralogy and establish the liberation size of the titanium-bearing phases; (ii) to evaluate the performance of high-intensity magnetic separation under reverse-beneficiation logic across a range of particle sizes and field intensities; and (iii) to characterise the resulting non-magnetic concentrate by XRD, so as to confirm the phase assemblage and provide a mineralogically grounded basis for subsequent metallurgical development.

2. Materials and methods

2.1. Ore sample and preparation

The titanium ore used in this study was collected from a primary hard-rock deposit in the Eskişehir region. The run-of-mine sample, with a maximum particle size of approximately 100 mm, was subjected to a three-stage comminution circuit consisting of primary jaw crushing, secondary cone crushing, and tertiary roll crushing, reducing all material to below 2 mm. The crushed product was riffle-split into representative sub-samples for chemical characterization and beneficiation experiments. Sieve analysis of the crushed product gave a P80 of approximately 1.0 mm.

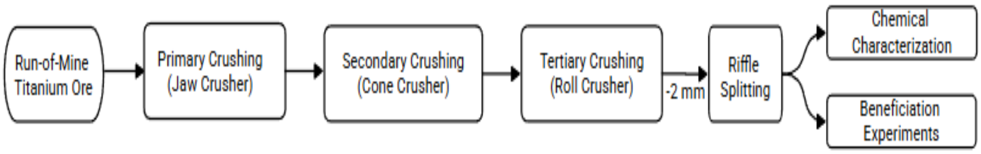

Fig. 1. Titanium ore sample preparation flowsheet

2.2. Characterization

The chemical composition of the ore was determined by X-ray fluorescence (XRF) spectrometry. For mineralogical characterization, polished and thin sections were examined under a reflected-light polarizing microscope to identify mineral phases, grain morphologies, and intergrowth textures. The mineralogical composition of the optimum concentrate was determined by powder X-ray diffraction using a Bruker D8 Advance diffractometer (Bruker, Karlsruhe, Germany) with Cu Kα radiation (λ = 1.5406 Å), operated at 40 kV and 40 mA. Data were collected over 2θ = 2–72° with a step size of 0.02° and a scan speed of 5° min^{-1}. Qualitative phase identification was carried out by matching the measured patterns against reference patterns of the ICDD PDF-2 database. Quantitative phase proportions were calculated in weight per cent by the reference intensity ratio (RIR) method; no Rietveld refinement was performed. The reported abundances are therefore semi-quantitative and are given as returned by the analysis, without normalisation to 100%, and an uncertainty of the order of ±2 wt% absolute should be assumed for the major phases.

2.3. Beneficiation experiments

The primary beneficiation method employed in this study is magnetic separation, based on the principle that titanium-bearing minerals exhibit markedly different magnetic susceptibilities from iron-bearing gangue minerals. Three different types of high-intensity magnetic separators were used throughout the experiments, selected according to the particle size range of each fraction: a dry rare-earth magnetic roll separator (REMS), a dry induced roll magnetic separator, and a Carpco wet high-intensity magnetic separator (WHIMS). Schematic views of these separators are presented in Fig. 2. Experiments were conducted in three systematic stages to evaluate the effects of liberation size and magnetic separation conditions on beneficiation performance.

Stage 1: The crushed −2 mm ore was wet-sieved into four narrow size fractions—−2+1.19 mm, −1.19+0.354 mm, −0.354+0.150 mm, and −0.150 mm—to maximize separation selectivity. The coarse fractions (−2+1.19 mm and −1.19+0.354 mm) were processed using a dry rare-earth magnetic roll separator (REMS) operated at its maximum field intensity of 11,000 Gauss (1.1 T). The intermediate fraction (−0.354+0.150 mm) was treated using a high-intensity dry induced roll magnetic separator operated at its maximum field intensity of 10,000 Gauss (1.0 T). The finest fraction (−0.150 mm) was processed in a Carpco wet high-intensity magnetic separator (WHIMS) operated at its maximum field intensity of 11,000 Gauss (1.1 T).

Stage 2: As the Stage 1 results indicated insufficient liberation at coarser sizes, the ore was ground to 100% passing 0.354 mm to improve liberation and separation selectivity. Grinding was performed in a laboratory ball mill at a 45% ball charge and 60% solids by weight in two 5-min grinding cycles, with screening to remove undersize material before the second cycle. The ground product was classified into three narrow size fractions—−0.354+0.212 mm, −0.212+0.106 mm, and −0.106 mm—and each fraction was processed in a two-stage magnetic separation circuit using the Carpco WHIMS at field intensities of 7,000 and 11,000 Gauss (0.7 and 1.1 T), respectively. Sieve analysis of this ground product gave a P80 of 0.24 mm, with 50% of the mass finer than approximately 0.07 mm.

Stage 3: For final process optimization, the crushed −2 mm ore was ground to 100% passing 0.106 mm under the same milling conditions but with an extended grinding time of two 10-min cycles, with screening to remove undersize material before the second cycle. The resulting pulp was processed in a two-stage wet magnetic separation circuit using the Carpco WHIMS at field intensities of 7,000 and 11,000 Gauss (0.7 and 1.1 T), respectively. The chemical compositions of all beneficiation products were determined by XRF analysis, and the concentrate yielding the highest TiO_2 grade was additionally characterized by XRD for mineralogical phase identification. Wet sieve analysis of the mill product gave a P80 of 0.046 mm, so that the material treated in Stage 3 was appreciably finer than its nominal 0.106 mm top size.

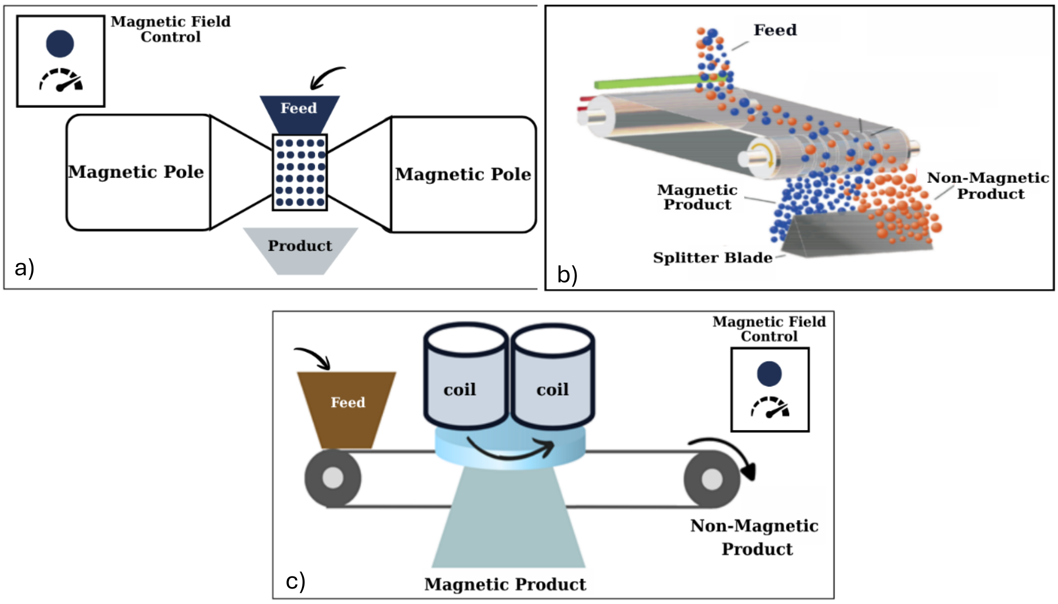

Fig. 2. Magnetic separators used in the beneficiation experiments: a) Carpco wet high-intensity magnetic separator (WHIMS), b) REMS dry rare-earth magnetic roll separator, c) dry induced roll magnetic separator

All grade and recovery values reported in Tables 2–4 are referenced to the reconstituted (calculated) feed of each test series rather than to the XRF head assay of Table 1, so that every mass balance closes internally. The reconstituted run-of-mine grades of 4.01, 3.93 and 4.02% TiO_2 deviate from the head assay of 4.07% TiO_2 by less than 3.5% relative, and the corresponding Fe_2O_3 values of 23.88, 23.97 and 23.77% deviate from 24.11% by less than 1.5% relative. The largest deviation occurs for CaO (10.74–10.85% against 11.38%, up to 5.6% relative), which is to be expected because carbonate is the most heterogeneously distributed phase in the ore and is therefore the most sensitive to sub-sampling. It should further be noted that the reconstituted values lie slightly below the head assay for all three oxides and in all three test series. This consistent direction is attributed to sub-sampling of a heterogeneous hard-rock feed together with a minor loss of fines during the wet separation and drying steps, in which the removed material is not recovered for assay. The effect is small and does not alter any of the trends reported here; the reconstituted feed is adopted as the reference basis throughout for this reason, whereas the head assay of Table 1 is retained as the compositional reference for the run-of-mine ore.

Each separation test reported here was carried out once; replicate separation tests were not performed, and the repeatability of the circuit has therefore not been determined directly. An indicative estimate of the combined variability arising from sub-sampling, processing and assay can nevertheless be obtained from the three reconstituted run-of-mine compositions given above, which derive from three independently prepared sub-samples of the same run-of-mine material processed in three separate test series. The corresponding standard deviations are 0.05% absolute for TiO_2, 0.10% for Fe_2O_3 and 0.06% for CaO, equivalent to relative standard deviations of 1.2%, 0.4% and 0.6% respectively. Because these values also contain the sub-sampling and processing contributions, they represent an upper bound on the analytical uncertainty rather than the precision of the XRF determination alone, and with only three determinations they should be regarded as indicative rather than as a formal repeatability estimate. On this basis, differences in TiO_2 grade smaller than approximately 0.1% absolute are not resolved by the present data set, and only larger differences are interpreted in the discussion that follows.

3. Results and discussion

3.1. Chemical and mineralogical composition of the feed ore

The chemical composition of the run-of-mine ore is presented in Table 1, and polarized light microscopy images of the Eskişehir titanium ore are given in Fig. 3. The ore contains 4.07% TiO_2 in a complex silicate-iron oxide matrix dominated by SiO_2 (36.09%) and Fe_2O_3 (24.11%), with significant CaO (11.38%), Al_2O_3 (10.21%), and MgO (4.58%). This geochemical signature—iron-rich, calcium-bearing, with elevated Mg and Al—is characteristic of a calc-silicate alteration assemblage associated with alkaline silicate-carbonatite intrusions subjected to extensive hydrothermal alteration. The high Fe_2O_3 content (24.11%) derives primarily from hematite and magnetite as gangue phases, which enable the reverse magnetic separation strategy described below.

Table 1. XRF chemical composition of the run-of-mine titanium ore

Oxide	TiO_2	SiO_2	Fe_2O_3	CaO	Al_2O_3	MgO	Other
Content (%)	4.07	36.09	24.11	11.38	10.21	4.58	9.56

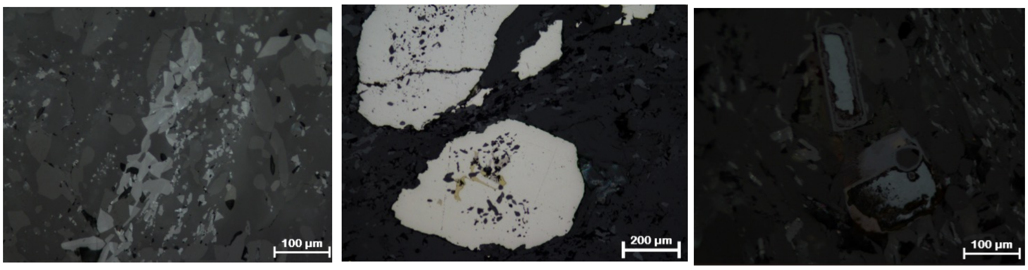

Fig. 3. Polarized light microscopy images of the titanium ore

As shown in Fig. 3, polarized light microscopy revealed a schistose rock texture with abundant sphene (titanite) and rutile grains clearly distinguishable. No sulfide minerals were identified beyond goethite-altered pyrite. Magnetite and ilmenite were present only in minor quantities. This mineralogical configuration—characterized by the dominance of non-magnetic titanite over paramagnetic ilmenite—constitutes the fundamental basis of the reverse beneficiation strategy employed in this work.

3.2. Magnetic separation tests

Systematic magnetic separation experiments on the crushed −2 mm feed, subdivided by wet sieving into four narrow size fractions and processed by REMS, induced roll, and Carpco separators, revealed a clear liberation-controlled beneficiation response (Table 2). The coarse fractions (−2+1.19 mm and −1.19+0.354 mm) showed essentially no TiO_2 upgrade: the non-magnetic products from these size classes achieved only 3.67% and 5.87% TiO_2, respectively, barely above the feed grade of 4.07%, confirming that titanite grains remain locked within the silicate-iron oxide matrix at these particle sizes and that the degree of liberation is insufficient for effective separation.

A meaningful but still modest upgrade was observed in the −0.354+0.150 mm fraction (non-magnetic grade 6.54% TiO_2) and the −0.150 mm fraction (non-magnetic grade 6.45% TiO_2), indicating the onset of liberation at approximately 0.354 mm. The two grades differ by only 0.09% TiO_2, which is comparable with the estimated variability of the measurements given in Section 2.3; the two fractions are therefore regarded as behaving equivalently, and the difference between them is not interpreted. These results are consistent with the fine-grained, intimately intergrown ore texture revealed by polarized light microscopy, and confirm that further size reduction is required to achieve adequate liberation for effective beneficiation. This indicates that titanium minerals can only be sufficiently liberated at particle sizes finer than 0.354 mm.

One limitation of the Stage 1 test series should be stated explicitly. The four size fractions were necessarily processed in three different machines, each chosen for the size range to which it is mechanically suited. The magnetic force acting on a particle scales with the product of the field intensity and the field gradient rather than with the field intensity alone, and the manner in which the gradient is generated differs fundamentally between the three units — permanent rare-earth rolls in the REMS, an induced-roll electromagnet, and a wire matrix in the WHIMS — as does the carrier medium, dry in the first two and wet in the third. The nominal field intensities quoted for Stage 1 are therefore not strictly comparable with one another, and within this stage the effect of particle size cannot be separated from the effect of separator type.

This limitation does not, however, affect the conclusion that liberation rather than field intensity governs the beneficiation response, because Stage 2 provides an independent test in which the separator is held constant. There, all three size fractions were processed in the same Carpco WHIMS at the same two field intensities of 7,000 and 11,000 Gauss, and the grade of the non-magnetic product rises monotonically as the size decreases, from 6.12% TiO_2 in the −0.354+0.212 mm fraction to 9.54% TiO_2 in the −0.212+0.106 mm fraction and 11.96% TiO_2 below 0.106 mm (Table 3). Expressed as enrichment ratios relative to the feed grade of each individual fraction, which removes the influence of differences in head grade between fractions, the same sequence gives 1.75, 2.23 and 3.00. The size effect is therefore established on a single machine under identical field conditions and is not an artefact of the separator sequence employed in Stage 1.

The same comparison also shows the Fe_2O_3 grade of the non-magnetic product falling from 17.89% to 9.75% and 5.90% over the same size sequence. This is significant because the alternative explanation — that the improvement with decreasing size reflects separator performance rather than liberation — would predict the opposite: since the magnetic force on a particle scales with its volume, fine paramagnetic particles are captured less efficiently and would report increasingly to the non-magnetic product, raising rather than lowering its iron content. The simultaneous increase in TiO_2 grade and decrease in Fe_2O_3 grade is therefore consistent only with progressive liberation.

Table 2. Magnetic separation test results for the −2 mm crushed ore processed in different magnetic separators according to size fraction

Size, mm	PRODUCT	Amount %	TiO_2		Fe_2O_3		CaO	
			G %	R %	G %	R %	G %	R %
-2+ 1.19 mm	Magnetic	15.9	4.73	18.8	19.54	13.0	10.25	15.2
	Non-magnetic	17.4	3.67	15.9	15.43	11.2	11.94	19.3
	Fraction Feed	**33.3**	**4.18**	**34.7**	**17.39**	**24.3**	**11.13**	**34.5**
-1.19+ 0.354 mm	Magnetic	13.2	3.77	12.4	31.86	17.6	10	12.3
	Non-magnetic	9.5	5.87	13.9	32.37	12.9	14.38	12.7
	Fraction Feed	**22.7**	**4.65**	**26.3**	**32.07**	**30.5**	**11.83**	**25.0**
-0.354+ 0.15 mm	Magnetic	10.6	2.35	6.2	41.98	18.6	7.80	7.7
	Non-magnetic	6.0	6.54	9.8	25.66	6.5	14.86	8.3
	Fraction Feed	**16.6**	**3.87**	**16.0**	**36.08**	**25.1**	**10.35**	**16.0**
-0.15 mm	Magnetic	21.7	2.53	13.7	19.80	18.0	8.93	18.0
	Non-magnetic	5.7	6.45	9.2	9.18	2.2	12.12	6.4
	Fraction Feed	**27.4**	**3.35**	**22.9**	**17.59**	**20.2**	**9.60**	**24.5**
RUN OF MINE		**100.0**	**4.01**	**100.0**	**23.88**	**100.0**	**10.74**	**100.0**

G: Grade; R: Recovery

A further significant finding derived from these beneficiation experiments concerns the mineralogical nature of the titanium-bearing phases in the ore. As evidenced by the results, TiO_2 consistently reports to the non-magnetic product upon upgrading, clearly indicating that the dominant titanium mineral in the ore does not possess magnetic properties. Among the primary titanium minerals, ilmenite ($FeTiO_3$) would be expected to report to the magnetic fraction due to its inherent magnetic susceptibility, whereas minerals such as rutile (TiO_2) and sphene ($CaTiSiO_5$), which contain no structural iron, exhibit no magnetic susceptibility and therefore report to the non-magnetic fraction. In light of these findings, it is concluded that the primary TiO_2-bearing mineral in this ore is rutile and/or sphene (titanite), while the ~2–2.5% TiO_2 in the fine-fraction magnetic products indicates that the ore also contains a minor proportion of ilmenite.

Based on the findings obtained from this set of experiments, the ore sample was ground to below 0.354 mm in order to enhance the degree of liberation and achieve a more selective separation. The ground product was classified into the narrow size fractions -0.354+0.212 mm, -0.212+0.106 mm, and -0.106 mm, and magnetic separation tests were carried out on each fraction; the corresponding results are presented in Table 3. Since both grinding and classification were performed under wet conditions, the beneficiation was conducted using a Carpco wet high-intensity magnetic separator (WHIMS).

Table 3. Magnetic separation test results of the ore ground to below 0.354 mm

Size, mm	PRODUCT	Amount %	TiO_2		Fe_2O_3		CaO	
			G %	R %	G %	R %	G %	R %
-0.354+0.212 mm	7000 Gauss Magnetic-1	13.9	3.07	10.8	26.76	15.5	8.63	11.1
	11000 Gauss Magnetic-2	10.6	3.61	9.7	21.80	9.6	8.84	8.7
	11000 Gauss Non-magnetic	1.8	6.12	2.8	17.89	1.4	11.11	1.9
	Fraction Feed	**26.3**	3.50	23.4	24.15	26.5	8.89	21.7
-0.212+0.106 mm	7000 Gauss Magnetic-1	7.7	2.76	5.4	28.47	9.1	7.26	5.2
	11000 Gauss Magnetic-2	10.4	3.33	8.8	14.50	6.3	14.39	13.9
	11000 Gauss Non-magnetic	4.1	9.54	10.0	9.75	1.7	14.70	5.6
	Fraction Feed	**22.2**	4.28	24.2	18.47	17.1	11.97	24.7
-0.106 mm	7000 Gauss Magnetic-1	37.0	2.65	25.0	31.34	48.4	10.22	35.1
	11000 Gauss Magnetic-2	7.7	3.48	6.9	19.64	6.3	10.35	7.4
	11000 Gauss Non-magnetic	6.8	11.96	20.6	5.90	1.7	17.85	11.2
	Fraction Feed	**51.5**	3.99	52.4	26.25	56.4	11.24	53.7
	RUN OF MINE	**100.0**	**3.93**	**100.0**	**23.97**	**100.0**	**10.74**	**100.0**

An examination of the magnetic separation results presented in Table 3 reveals that progressively higher TiO_2 grades are achieved as the particle size decreases, owing to the improved liberation of the titanium-bearing minerals. In the −0.354+0.212 mm size fraction, a non-magnetic product accounting for 1.8% of the mass was obtained at a grade of 6.12% TiO_2; in the −0.212+0.106 mm fraction the non-magnetic product accounted for 4.1% of the mass at a grade of 9.54% TiO_2, whereas reducing the particle size below 0.106 mm yielded a non-magnetic product representing 6.8% of the mass at a higher grade of 11.96% TiO_2. This trend indicates that the liberation of the titanium-bearing minerals occurs predominantly at sizes finer than 0.106 mm.

It should be emphasised that the threshold identified here is an operational one, inferred from the grade–size trend of the separation products rather than measured directly. The term is used in this paper to denote the size below which the titanium-bearing phases become sufficiently detached from the gangue for magnetic separation to be effective, and not a quantified degree of liberation. A direct determination by automated mineralogy, for example MLA or QEMSCAN, would be required to establish the true liberation distribution and is recommended for future work on this ore.

The higher TiO_2 grades obtained from the beneficiation of the ore below 0.106 mm indicate that the degree of liberation increases markedly at sizes finer than this threshold. Accordingly, the entire ore sample was ground to below 0.106 mm and subjected directly to beneficiation using the Carpco wet high-intensity magnetic separator (WHIMS); the corresponding results are presented in Table 4.

Processing the fully ground (−0.106 mm) feed in the wet high-intensity circuit produced the best results. The TiO_2 grade of the non-magnetic concentrate increased significantly from 4.07% in the ROM ore to a peak of 12.78%, while the overall titanium recovery in this product reached 53.7%. The two-stage magnetic separation system successfully rejected 95.4% of the total iron into the tailings. The initial

7,000 Gauss stage removed the bulk of the gangue mass (60.8%), consisting mainly of iron oxides, whereas the subsequent 11,000 Gauss scavenger stage effectively removed the moderately locked particles and liberated ilmenite, as reflected by its slightly higher TiO_2 grade of 2.98%. To reveal the mineralogy of the titanium concentrate containing 12.78% TiO_2, XRD analysis was performed, and the resulting X-ray diffractogram is presented in Fig. 4.

Table 4. Magnetic separation test results of the ore ground to below 0.106 mm

Size, mm	PRODUCT	Amount %	TiO_2		Fe_2O_3		CaO	
			G %	R %	G %	R %	G %	R %
-0.106 mm	7000 Gauss Magnetic-1	60.8	1.97	29.8	30.87	79.0	7.98	44.7
	11000 Gauss Magnetic-2	22.3	2.98	16.5	17.5	16.4	12.34	25.4
	11000 Gauss Non-magnetic	16.9	12.78	53.7	6.5	4.6	19.23	29.9
	Fraction Feed	100.0	4.02	100.0	23.77	100.0	10.85	100.0

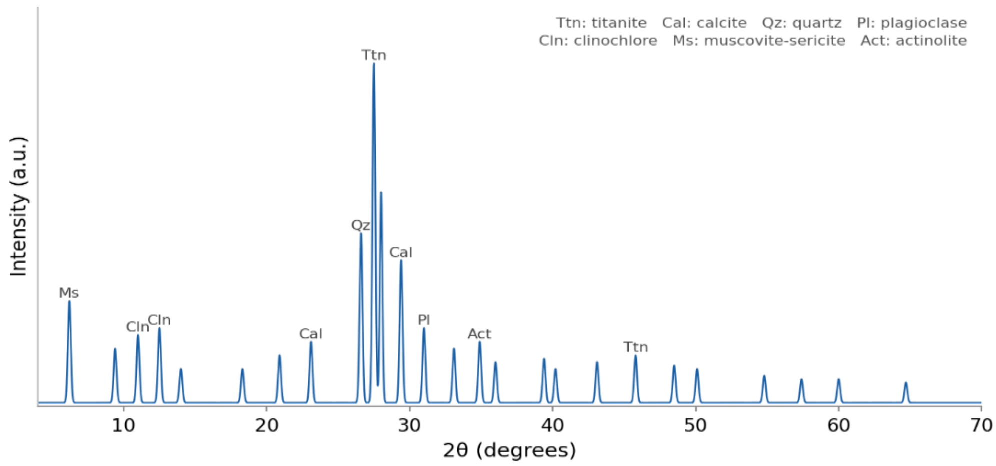

Fig. 4. X-ray diffractogram of the non-magnetic concentrate (Ttn: titanite, Cal: calcite, Qz: quartz, Pl: plagioclase, Cln: clinochlore, Ms: muscovite-sericite, Act: actinolite)

The semi-quantitative XRD analysis confirmed the phase composition of the optimized concentrate, indicating that titanite (sphene, $CaTiSiO_5$) was the main titanium-bearing phase in the non-magnetic product (23.9 wt%). The remaining mass consisted of liberated gangue minerals entrained in the non-magnetic product: calcite (18.6%), quartz (11.7%), plagioclase feldspar (11.4%), clinochlore (11.3%), muscovite-sericite (9.2%), and actinolite (5.7%). The phases identified account for 94.9 wt% of the concentrate; the remaining 5.1 wt% corresponds to unidentified minor phases and to the background contribution of the semi-quantitative procedure. The abundances have deliberately not been renormalised to 100%, so that the values discussed below are those actually returned by the analysis. The analysis also showed that the ilmenite content of the concentrate was only 3.1%, demonstrating that the 11,000 Gauss magnetic field was highly efficient at isolating the non-iron-bearing titanium minerals (Fig. 5). Producing a concentrate with approximately 13% TiO_2 by physical magnetic separation alone establishes an effective pre-concentration route for Eskişehir primary ores, significantly reducing the mass of material requiring subsequent intensive hydrometallurgical or flotation processing.

The stoichiometric TiO_2 mass balance of the optimised non-magnetic concentrate provides further insight into the mineralogical composition of the product. Based on stoichiometric calculations, the titanite content of 23.9 wt% accounts for approximately 9.75% TiO_2 (using a TiO_2/titanite ratio of 0.408), while the ilmenite content of 3.1 wt% contributes a further 1.63% TiO_2 (TiO_2/ilmenite ratio of 0.526), yielding a combined total of approximately 11.38% TiO_2 from these two phases. The measured concentrate grade of 12.78% TiO_2 (by XRF) implies a residual contribution of approximately 1.40% TiO_2 attributable to rutile—consistent with the rutile grains identified in the feed ore by polarized light microscopy. The absence of a discrete rutile peak in the XRD diffractogram is explained by the very low proportion of this phase in the concentrate, which falls below the practical detection limit of conventional powder XRD (typically 1–2 wt%). This interpretation is fully consistent with the microscopic observations and confirms that the titanium mineralogy of the non-magnetic product is dominated by titanite, with subordinate ilmenite and trace rutile.

The calcium content of the concentrate deserves separate comment. Applying to CaO the same stoichiometric approach used above for TiO_2, calcite (18.6 wt%) accounts for 10.42% CaO and titanite (23.9 wt%) for a further 6.84%, with the remainder attributable to the plagioclase and actinolite; the sum reproduces the measured value of 19.23% CaO and thereby provides an independent check on the consistency of the XRD and XRF data. Calcium is therefore not held predominantly in carbonate, as the bulk grade might suggest: little more than half resides in calcite, whereas roughly one third is structurally bound within titanite itself. The calcite fraction is in principle removable, for example by reverse flotation, and its rejection would lower the acid demand of any subsequent leaching step. The calcium hosted in titanite, by contrast, cannot be rejected by physical means without also rejecting the titanium, so that a substantial residual CaO content is an intrinsic characteristic of a titanite-based concentrate rather than a deficiency of the separation. This is relevant to the selection of the downstream route, since feedstocks with high calcium and magnesium contents are unsuitable for the chloride process (Gázquez et al., 2014).

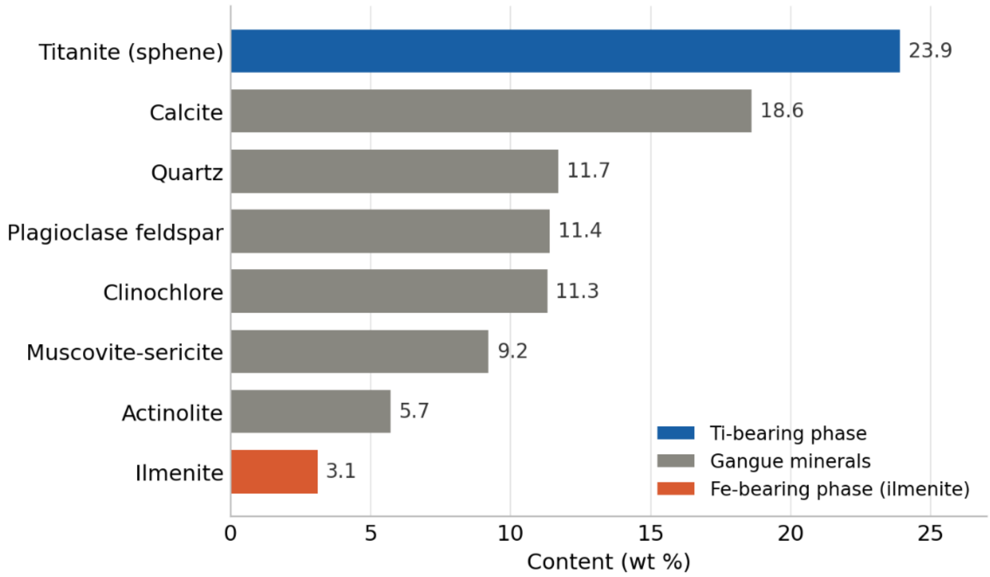

Fig. 5. XRD phase composition of the optimized non-magnetic concentrate (12.78% TiO_2)

4. Conclusions

This study presents the first systematic physical beneficiation investigation of a representative hard-rock titanium ore from the Eskişehir primary deposit, and the following conclusions can be drawn:

The run-of-mine ore contains 4.07% TiO_2 within a complex silicate–iron oxide matrix dominated by SiO_2 (36.09%) and Fe_2O_3 (24.11%). Polarized light microscopy revealed a schistose texture in which titanite (sphene) and rutile occur as the principal titanium-bearing phases, with magnetite and ilmenite present only in minor amounts. The dominance of non-magnetic titanite over paramagnetic ilmenite established the mineralogical basis for a reverse magnetic separation strategy.

Magnetic separation tests demonstrated a strongly liberation-controlled beneficiation response. Coarse fractions (above 0.354 mm) showed essentially no upgrading, with non-magnetic products barely exceeding the feed grade, confirming that the titanium-bearing minerals remain locked within the gangue matrix at these sizes. An operational liberation threshold, inferred from the marked rise in non-magnetic TiO_2 grade with decreasing size, was reached only below 0.106 mm; a quantitative liberation analysis (e.g. automated mineralogy) is recommended to confirm this threshold directly.

Under optimum conditions—ore ground to 100% passing 0.106 mm and processed in a two-stage Carpco WHIMS circuit at 7,000 and 11,000 Gauss—a non-magnetic titanium concentrate grading 12.78% TiO_2 was obtained at a recovery of 53.7%, representing an approximately threefold upgrade from the feed. The two-stage circuit rejected 95.4% of the total iron into the magnetic tailings. The remaining titanium reported mainly to the first (7,000 Gauss) magnetic stage as fine, incompletely liberated titanite locked with iron-bearing gangue; this loss defines the principal target for further optimisation of the comminution and circuit configuration. The result should therefore be regarded as a pre-concentration outcome that rejects about 83% of the feed mass without reagents, rather than as a finished concentrate, with the recovery–grade trade-off to be tuned according to the requirements of the downstream metallurgical route.

Semi-quantitative XRD analysis of the optimum concentrate confirmed titanite (23.9 wt%) as the dominant titanium-bearing phase, with ilmenite limited to only 3.1%, demonstrating the high selectivity of the reverse magnetic separation approach in isolating non-iron-bearing titanium minerals.

Overall, the production of a ~13% TiO_2 concentrate by physical magnetic separation alone establishes an effective, reagent-free pre-concentration route for Eskişehir primary titanium ores. This significantly reduces the mass of material requiring subsequent intensive hydrometallurgical or flotation processing and provides a mineralogically grounded basis for the further metallurgical development of Türkiye's domestic hard-rock titanium resources.

Acknowledgments

This study was supported by the Istanbul Technical University Scientific Research Projects Unit (Project No. MAB-2021-42889 and MGA-2021-42888). The authors gratefully acknowledge the Department of Mineral Processing Engineering at Istanbul Technical University for their valuable contributions to the realization of this work.

References

CHEN, Q., KASOMO, R.M., LI, H., JIAO, X., ZHENG, H., WENG, X., MUTUA, N.M., SONG, S., HE, D., LUO, H., 2021. *Froth flotation of rutile – An overview.* Miner. Eng. 163, 106797. https://doi.org/10.1016/j.mineng.2021.106797

ERSOY, Y.E., YAVUZ, H., UYSAL, İ., PALMER, M.R., MÜLLER, D., 2025. *The petrology of tuffisite in a trachytic diatreme from the Kızılcaören alkaline silicate–carbonatite complex, NW Anatolia.* Minerals 15(8), 867. https://doi.org/10.3390/min15080867

EUROPEAN COMMISSION, 2024. *Regulation (EU) 2024/1252 of the European Parliament and of the Council of 11 April 2024 establishing a framework for ensuring a secure and sustainable supply of critical raw materials (Critical Raw Materials Act).* Official Journal of the European Union, OJ L, 2024/1252.

EUROPEAN COMMISSION, JOINT RESEARCH CENTRE, BUESA, A., GEORGITZIKIS, K., JAKIMÓW, M., PIÑERO, P., MAURY, T., LATUNUSSA, C., PEDAUGA, L., SAMOKHVALOV, V., BALDASSARRE, B., MATHIEUX, F., RUEDA-CANTUCHE, J.M., STIJEPIC, D., REYS, A., BILOUS, A., NOTOM, P., TERCERO, L., 2025. *Titanium metal in the EU: Strategic relevance and circularity potential.* Publications Office of the European Union, Luxembourg, JRC137082. https://doi.org/10.2760/5871804

FAWZY, M.M., SHAWKY, M.M., ISMAIL, A.M., BAYOUMI, M., SHAHIN, H., EMAD, B., ORABI, A.H., ALY, G.A.M., ABDELMOUTY, A.M., DIAB, M., 2025. *Optimized and sustainable recovery of ilmenite and titanite from low-grade Rahba placer deposits: Integrating physical beneficiation techniques.* J. Min. Environ. 16(6), 1897–1912. https://doi.org/10.22044/jme.2025.16225.3141

GÁZQUEZ, M.J., BOLÍVAR, J.P., GARCIA-TENORIO, R., VACA, F., 2014. *A review of the production cycle of titanium dioxide pigment.* Mater. Sci. Appl. 5(7), 441–458. https://doi.org/10.4236/msa.2014.57048

LIU, Y., LIU, Z., WANG, Y., ZHANG, Y., LU, D., 2025. *Mineralogical analysis of factors affecting the grade of high-gradient magnetic separation concentrates and experimental study on TiO_2 enrichment using ARC.* Minerals 15(8), 799. https://doi.org/10.3390/min15080799

NATO, 2024. *NATO releases list of 12 defence-critical raw materials.* North Atlantic Treaty Organization, 11 December 2024. https://www.nato.int/cps/en/natohq/news_231765.htm (accessed 10 July 2026)

NZEH, N.S., POPOOLA, P.A., OKANIGBE, D., ADEOSUN, S., ADELEKE, A., 2023. *Physical beneficiation of heavy minerals – Part 1: A state of the art literature review on gravity concentration techniques.* Heliyon 9(8), e18919. https://doi.org/10.1016/j.heliyon.2023.e18919

NZEH, N.S., POPOOLA, P.A., 2024. *Physical beneficiation of heavy minerals – Part 2: A state of the art literature review on magnetic and electrostatic concentration techniques.* Heliyon 10(11), e32201. https://doi.org/10.1016/j.heliyon.2024.e32201

OPALEV, A.S., FOMIN, A.V., ALEKSEEVA, S.A., KALIUZHNAIA, R.V., 2026. *Application of magnetic-and-gravity separation in production of titanomagnetite concentrates from ores of various Russian deposits.* Russ. Min. Ind. 1, 89–96. https://doi.org/10.30686/1609-9192-2026-1-89-96